Journal of Traditional and Complementary Medicine 14 (2024) 287–299

Contents lists available at ScienceDirect

Journal of Traditional and Complementary Medicine

journal homepage: www.elsevier.com/locate/jtcme

Betanin combined with virgin coconut oil inhibits neuroinflammation in aluminum chloride-induced toxicity in rats by regulating NLRP3 inflammasome

Baban S. Thawkar, Ginpreet Kaur *

Department of Pharmacology, SPP School of Pharmacy & Technology Management, SVKM's NMIMS, V.L. Mehta Road, Vile Parle (W), Mumbai, 400056, India

ARTICLE INFO

Keywords:
Medium-chain triglycerides
NLRP3
Amyloid beta
Mitochondrial dysfunction
IL-1β
Brain glucose hypometabolism

ABSTRACT

Background and aim: Activating NLRP3 (NOD-, LRR-, and pyrin domain-containing protein 3) is crucial in the pathogenesis of Alzheimer's disease (AD). A multimodal treatment intervention is the most feasible way to alter the course of AD progression. Hence, the current study was conducted to study the combination of betanin (BET) and virgin coconut oil (VCO) on NLRP3 regulation in aluminum chloride-induced AD in Wistar rats.

Experimental procedure: BET (100,200 mg/kg) and VCO (1, 5 g/kg) alone and in combination (BET 100 mg/kg + VCO 1 g/kg and BET 200 mg/kg + VCO 5 g/kg) were given orally for 42 days. On day 21 and 42nd, the behavioral test was performed to check the animal's cognition. Acetylcholinesterase (AChE) activity, oxidative stress markers, estimation of NLRP3 and IL-1β, and histological examinations were conducted in the hippocampus (H) and cortex (C).

Results and conclusion: Treatment with BET and VCO alone or combined improved behavioral characteristics (MWM and PA $p < 0.0001$; EPM $p = 0.5184$), inhibited AChE activity (C, $p = 0.0101$; H, $p < 0.0001$), and lowered oxidative stress in the brain. Also, combination treatment restored the levels of NLRP3 (C, $p = 0.0062$; H, $p < 0.0001$) and IL1β (C, $p = 0.0005$; H, $p = 0.0098$). The combination treatment significantly reduced the degree of neuronal degeneration, amyloid deposition, and necrosis in the brain tissue. The current study revealed that the combination strategy effectively controlled neuroinflammation via modulation of the NLRP3 inflammasome pathway, paving the way for the new treatment.

1. Introduction

NLRP3 (NOD-, LRR- and pyrin domain-containing protein 3) is a 115 kDa cytosolic protein with three domains: a C-terminal leucine-rich repeat (LRR), a central nucleotide-binding and oligomerization domain NACHT, and an N-terminal pyrin domain (PYD).[1] Microparticles, ATP, cholesterol, and microbial toxins activate NLRP3. IL-1β causes synaptic loss via presynaptic glutamate release and post-synaptic NMDA (N-methyl-D-aspartate) receptor activation. In AD patients, elevated levels of inflammatory cytokines (IL-1β, IL-18, etc.) are prevalent. The inflammasome is becoming a crucial determinant in the development of mature IL-1β.[2] IL-1β is released from the microglial cell by activating TLR 4 (Toll-like receptors 4) via NF-κB and another by inflammasome complex activation. Both mechanisms contribute equally to the initiation of neuroinflammation by microglial activation.[3] NLRP3 activation occurred in two stages. Inflammasome assembly is produced by NF-kB-induced overexpression and a conformational shift in NLRP3.[4] Mitophagy, an autophagy-based stress response system, deals with the selective removal of damaged mitochondria. Hippocampal neurons in old mice show a 70 % decrease in mitophagy events, indicating its significance in neurodegenerative diseases.[5,6] Dysfunction in autophagy can cause diseases with increased NLRP3 inflammasome activation and act as a modulator of inflammasomes in neurodegenerative disorders.[7]

Ketone bodies (KBs) are considered an alternate energy source in mild cognitive impairment (MCI) conditions caused by brain glucose hypometabolism.[8] It also controls the regulation of glutamate. Thus, we could slow the progression of the disease by regulating neuroinflammation and energy hypometabolism. Because only symptom-modifying therapy is now available, a novel therapeutic

Peer review under responsibility of The Center for Food and Biomolecules, National Taiwan University.

* Corresponding author. Department of Pharmacology, SPP School of Pharmacy & Technology Management, SVKM's NMIMS, V.L. Mehta Road, Vile Parle (W), Mumbai, 400056, India.

E-mail address: Ginpreet.Kaur@nmims.edu (G. Kaur).

https://doi.org/10.1016/j.jtcme.2023.11.001
Received 27 August 2022; Received in revised form 27 October 2023; Accepted 5 November 2023
Available online 11 November 2023

List of abbreviations

AChE	Acetylcholinesterase enzyme
AD	Alzheimer's disease
BET	Betanin
CAT	catalase
EPM	Elevated Plus Maze
FID	Flame ionization detector
GC-MS	Gas chromatography-mass spectroscopy
GSH	Reduced glutathione
IL-1β	Interleukin-1 beta
LRR	a C-terminal leucine-rich repeat
MDA	Malondialdehyde
MWM	Morris Water Maze
NLRP3	NOD-, LRR- and pyrin domain-containing protein 3
PA	Passive avoidance
PMS	A post-mitochondrial supernatant
PNS	Post-nuclear supernatant
PYD	an N-terminal pyrin domain
SOD	superoxide dismutase
TLR 4	Toll-like receptors 4
VCO	Virgin coconut oil

strategy for AD is essential.

Betanin (BET) (betanidin 5-O-β-D-glucoside, red) is one of the betalains which comprises 75–95 % of total betalain obtained from *Beta vulgaris* (Family Caryophyllales) and is extensively cultivated and utilized as a health food.[9] It has excellent potential in diseases associated with oxidative stress and chronic inflammation, especially liver disease, arthritis, and cancer.[10] Several studies have found betalains to have high antioxidant, radioprotective, and anti-inflammatory activities *in vitro* and in several *in vivo* animal models.[11]

VCO (Virgin coconut oil) is usually obtained from the fresh coconut fruit of the plant *Cocos nucifera*. This oil is a valuable source of ketone bodies.[12] VCO diet or supplementation prevented rats from gentamicin nephrotoxicity, cadmium-induced nephrotoxicity, and levodopa neurotoxicity. A 4-week VCO supplement (30 mL/day) in young, healthy people enhances vascular endothelial function.[13] When used in conjunction with other medications, virgin coconut oil supplementation was proven to be beneficial. Its combination with licorice extract prevents hyperlipidemia and hepatosteatosis by inhibiting animal hepatic lipid production.[14] Coconut oil, in particular, has been claimed to mitigate the cognitive deficits linked with amyloid-β and aluminum chloride-induced AD in rats.[15]

Because of the complex pathophysiology of AD, combination therapies may be required rather than monotherapy.[16] Combining betanin and VCO can manage neuroinflammation and control glucose hypometabolism by supplying ketone bodies. As a result, the current study focused on employing an integrated strategy to target the unique NLRP3 pathway.

2. Material and methods

2.1. Drugs and chemicals

Betanin (Red Beet extract diluted with Dextrin, CAS 7659-95-2, TCI chemicals) and Max Care Virgin Coconut Oil (Cold Pressed) were purchased. Donepezil hydrochloride was procured from Micro Labs Limited, Mumbai, India. Aluminum chloride was procured from Sigma Aldrich (St. Louis, MO, USA). The rest of the chemicals were of analytical grade.

2.2. Characterization of virgin coconut oil

The fatty acid contents of the VCO have been evaluated by the Gas Chromatography Varian-CP-3800 (Varian, Inc., CA, USA) supplied with a flame ionization detector (FID) and a CP-Sil-88 column with a length of 100 m and a split ratio of 10:1 was used. According to the standards, the resultant picks and retention time (Rt) were compared to find fatty acids.[15]

2.3. Animal

Seventy-two male Albino Wistar rats (180–220 g) were acquired from the National Institute of Biosciences, Pune, India. Animals were kept in polypropylene cages at 12/12 h light/dark cycle at room temperature of 25 ± 2 °C, 40–60 % relative humidity. Animals had access to a standard pellet diet and water *ad libitum*. Before the experiment, the animals were conditioned for one week. The study protocol was approved through the Institutional Animal Ethics Committee (approval no. CPCSEA/IAEC/P-24/2018 dated September 6, 2018), which was formed by the norms of the Committee for the Purpose of Control And Supervision of Experiments on Animals (CPCSEA), Government of India.

2.4. Acute toxicity study as per the OECD guideline 423

The acute toxicity studies of the combination were performed according to Organization of Economic Corporation Development Guidelines No. 423 using SD female rats. BET (2000 mg/kg) and VCO (10 g/kg) were administered orally in a group of rats, and the percentage of mortality was recorded. The animals were monitored for the next 14 days with the prescribed doses for mortality or gross abnormalities. Depending on the acute toxicity test, BET oral dosages of 100 and 200 mg/kg and VCO doses of 1 and 5 g/kg were selected for the study.[17]

2.5. Experimental design

The seventy-two male albino Wistar rats (180–220 g) were selected based on body weight in nine groups of 8 animals each. We dissolved BET (100 and 200 mg/kg orally) and aluminum chloride (100 mg/kg) in millipore water, while VCO (1 and 5 g/kg orally) was administered in its natural form.

Group I received distilled water as a control, while Group II received aluminum chloride treatment at 100 mg/kg.[18,19] BET (100 and 200 mg/kg orally) was administered with aluminum chloride as Group III and IV, respectively. VCO (1 and 5 g/kg orally) was given along with aluminum chloride as Group V and VI, respectively. The combination group (BET 100 mg/kg + VCO 1 g/kg, BET 200 mg/kg + VCO 5 g/kg) was given along with aluminum chloride as Group VII and VIII. The standard group received Donepezil hydrochloride at 1 mg/kg, along with aluminum chloride as Group IX.

The animals in Groups III to IX were given aluminum chloride for 42 days. The drug treatment was administered to the rats after 1 h. On days 21 and 42, the rats underwent behavioral testing, which included training and probing tests. The rat cortex and hippocampus were separated for further biochemical and molecular research.

2.6. Behavioral assessment

2.6.1. Morris water maze (MWM)

This test is designed to determine spatial memory skills in rats. It was carried out as per the previous procedure but with minor changes. A big round swimming tank (150 cm diameter, 45 cm height) with four equal quadrants (NW, NE, SE, and SW) filled with water at 25 ± 1 °C. Red and blue colored tapes (symbols of " × " and "+") were used to generate visual clues surrounding the water tank to aid spatial orientation in experimental rats, and the positions of the cues were uniform throughout the experiment. During the acquisition phase, the

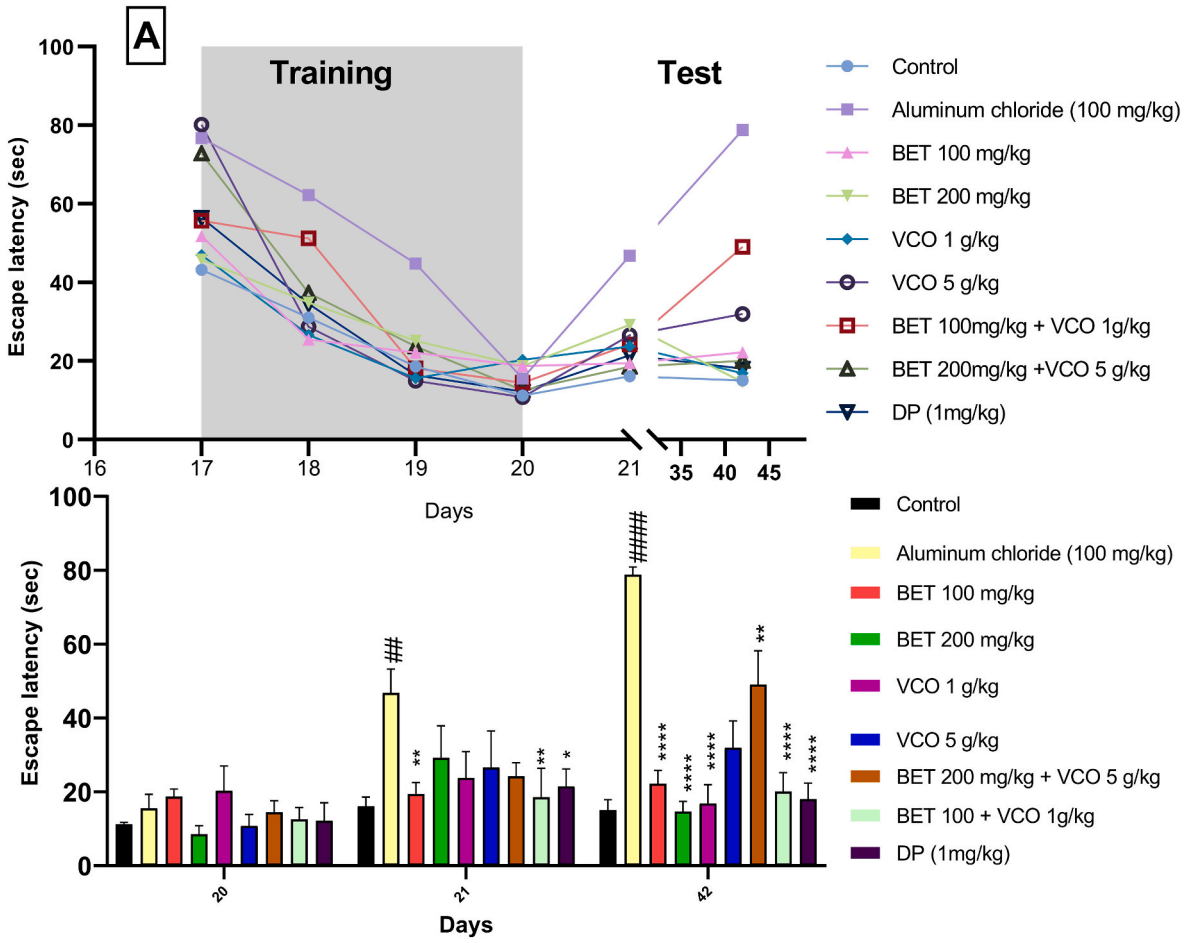

Fig. 1. Behavioral test of BET and VCO Morris water maze A) Training B) Test, Data are expressed as mean ± SEM, $^{\#\#\#\#}p < 0.0001$, $^{\#\#\#}p < 0.001$, $^{\#}p < 0.05$ when compared with normal control, ****$p < 0.0001$ ***$p < 0.001$**$p < 0.01$,*$p < 0.05$ when compared to treatment group.

submerged platform (10 * 10 cm) was kept 1 cm above the water's surface. The animal was put in the tank with its face to the wall. The animal was allowed to give 120 s to reach the platform. If the animal did not get to the platform within 120 s, it was directed to it and given 30 s on the platform. Training phase: each animal underwent four trials for four subsequent days (17th to 20th day) with a 10-min gap between sessions. During the retention phase or probe trial (on the 21st and 42nd day), the water surface was made cloudy using milk powder to mask the platform and kept 1 cm underneath the tank's water level. On days 21 and 42, the animal's memory retention was assessed. Escape latency was calculated by measuring the time to locate the animal's hidden platform in the water maze.[20]

2.6.2. *Elevated plus maze (EPM)*

The EPM is used to measure rodent cognitive function and was carried out in the same manner as previously described. The elevated plus-maze apparatus comprised two covered walls (50 * 10 cm), a cross with two open arms of the same size, and 40 cm high walls. Two arms of the EPM were attached to the central square (10*10 cm) and elevated 50 cm above the ground. During the acquisition test, the animal was put at one end of the arm, facing away from the central square region. Initial transfer latency (ITL) was noted as the time required for the animal to move from the open to the closed arm. Before returning to its home cage, each animal was encouraged to explore the maze for 20 s. Memory retention was assessed after 24 h, and the first and second transfer latency were measured on days 21 and 42, respectively.[21]

2.6.3. *Passive avoidance test (PA)*

This test is used to measure rodent memory retention impairments and was carried out using the previously described procedure. The apparatus was made up of a wooden box with a metal grid. It consists of light and dark compartments (25 * 25 * 25 cm each), supplied with a 40W lamp and divided by a guillotine door. The bottom of the dark container has a metal grid floor with a shock generator to provide electric shocks. The animal was put in the light chamber for 60 s during the acquisition test. The latency to walk inside the dark compartment after the guillotine door was opened was reported as pre-shock latency. After entering the dark chamber, the animal was administered a minor electric shock (0.5 mA for 2 s) through the grid floor, removed, and returned to the home cage. The rat was exposed to a retention test on the next day and the 42nd day, in which no electric shock was provided to the animal. The time to step into the dark compartment was recorded as post-shock latency in seconds.[22]

2.7. *Biochemical parameters*

2.7.1. *Collection of brain tissues*

Animals sacrificed by CO_2 asphyxiation. The hippocampus and cortex were separated from the brain. A probe homogenizer (Polytron PT 2500E, Kinematica, Switzerland) was used to homogenize 100 mg of tissue in 0.5 ml phosphate buffer (0.1 M, pH 7.4). The tubes were put on ice to eliminate temperature fluctuations and then stored at −80 °C. Different portions of tissue homogenates were produced and processed to yield post-nuclear and post-mitochondrial fractions.

Table 1
Effect of Combination on brain oxidative stress parameters in the hippocampus.

Group	MDA (nmol per mg protein)	GSH (μmol per mg protein)	SOD (U per mg protein)	CAT (nmol of H2O2 decomposed per min per mg protein)
Control	1.172 ± 0.11	7.617 ± 0.73	0.088 ± 0.021	15.67 ± 0.96
Aluminum chloride ($AlCl_3$)	2.393 ± 0.38$^{\#\#}$	1.086 ± 0.56$^{\#\#}$	0.041 ± 0.006$^{\#\#}$	9.019 ± 1.11$^{\#\#}$
$AlCl_3$ + BET 100 mg/kg	1.895 ± 0.40	5.911 ± 0.76	0.086 ± 0.007**	14.11 ± 1.70*
$AlCl_3$ + BET 200 mg/kg	1.421 ± 0.32	5.4 ± 0.30	0.081 ± 0.005**	14.29 ± 1.70*
$AlCl_3$ + VCO 1 g/kg	1.366 ± 0.16*	6.56 ± 1.74*	0.060 ± 0.002	14.67 ± 1.59*
$AlCl_3$ + VCO 5 g/kg	1.318 ± 0.24*	5.619 ± 0.82	0.069 ± 0.0009	12.91 ± 1.07
$AlCl_3$ + BET 100 mg/kg and VCO 1 g/kg	1.298 ± 0.14*	5.272 ± 2.30	0.058 ± 0.005	14.37 ± 1.10*
$AlCl_3$ + BET 200 mg/kg and VCO 5 g/kg	1.418 ± 0.09*	6.32 ± 1.94*	0.067 ± 0.003	14.03 ± 1.11
$AlCl_3$ + Donepezil HCl (1 mg/kg)	1.541 ± 0.12	5.579 ± 1.27	0.058 ± 0.003	13.91 ± 1.04

Data are expressed as mean ± S. E. M. (n = 6), $^{\#\#}p < 0.01$ when compared with normal control, **p < 0.01, *p < 0.05 when compared with disease control group.

2.7.2. Determination of acetylcholinesterase activity

According to the manufacturer's instructions, the Amplite™ Colorimetric acetylcholinesterase assay Kit was used to evaluate AChE activity. The reaction is initiated with the substrate acetylthiocholine. The DTNB dianion's production was measured at 412 nm within 10 min using a microplate reader.[23]

2.7.3. Determination of the oxidative stress parameters

Malondialdehyde (MDA) and reduced glutathione (GSH) assay were evaluated in the whole homogenate.[24,25] Post-nuclear supernatant (PNS) was obtained by centrifugation at 2500 rpm for 20 min at 4 °C. The catalase's activity was measured using PNS.[26] A post-mitochondrial supernatant (PMS) was used to test for superoxide dismutase (SOD) activity. It was formed by centrifuging homogenate for 20 min at 4 °C at 10,000 rpm.[27]

2.7.4. Estimation of IL 1-β level

The IL-1β level was determined using a commercially available GENLISA™ ELISA kit (Krishgen Biosystems, India) per the manufacturer's instructions. The absorbance was read at 450 nm within 10–15 min.

2.7.5. Estimation of NLRP3 level

To determine NLRP3, a commercially available Rat Nod-like Receptor Pyrin-3, NLRP3 GENLISA™ ELISA (Krishgen Biosystems, India), was used per the manufacturer's instructions. The absorbance was read at 450 nm within 10–15 min, and the results were exhibited as nanograms (ng) per milligram (mg) of tissue.

2.7.6. Protein determination

The total protein was quantified for the biochemical studies using the Bradford method with bovine serum albumin as a reference compound. A protein estimation kit was used to perform the estimation. (HI Media Laboratories, India).

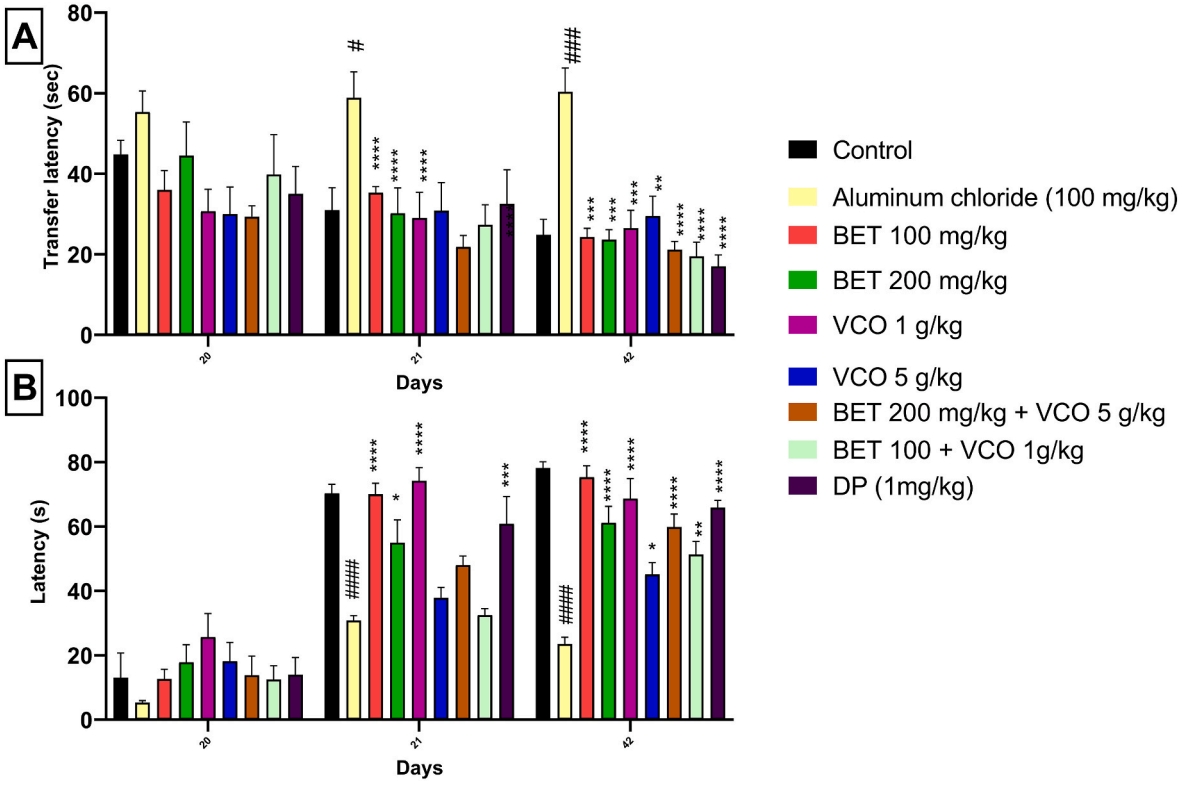

Fig. 2. Behavioral test of BET and VCO A) Elevated plus-maze B) Passive avoidance test. Data are expressed as mean ± SEM, $^{\#\#\#\#}p < 0.0001$, $^{\#\#}p < 0.01$ when compared with normal control, ****p < 0.0001 ***p < 0.001**p < 0.01,*p < 0.05 when compared to treatment group.

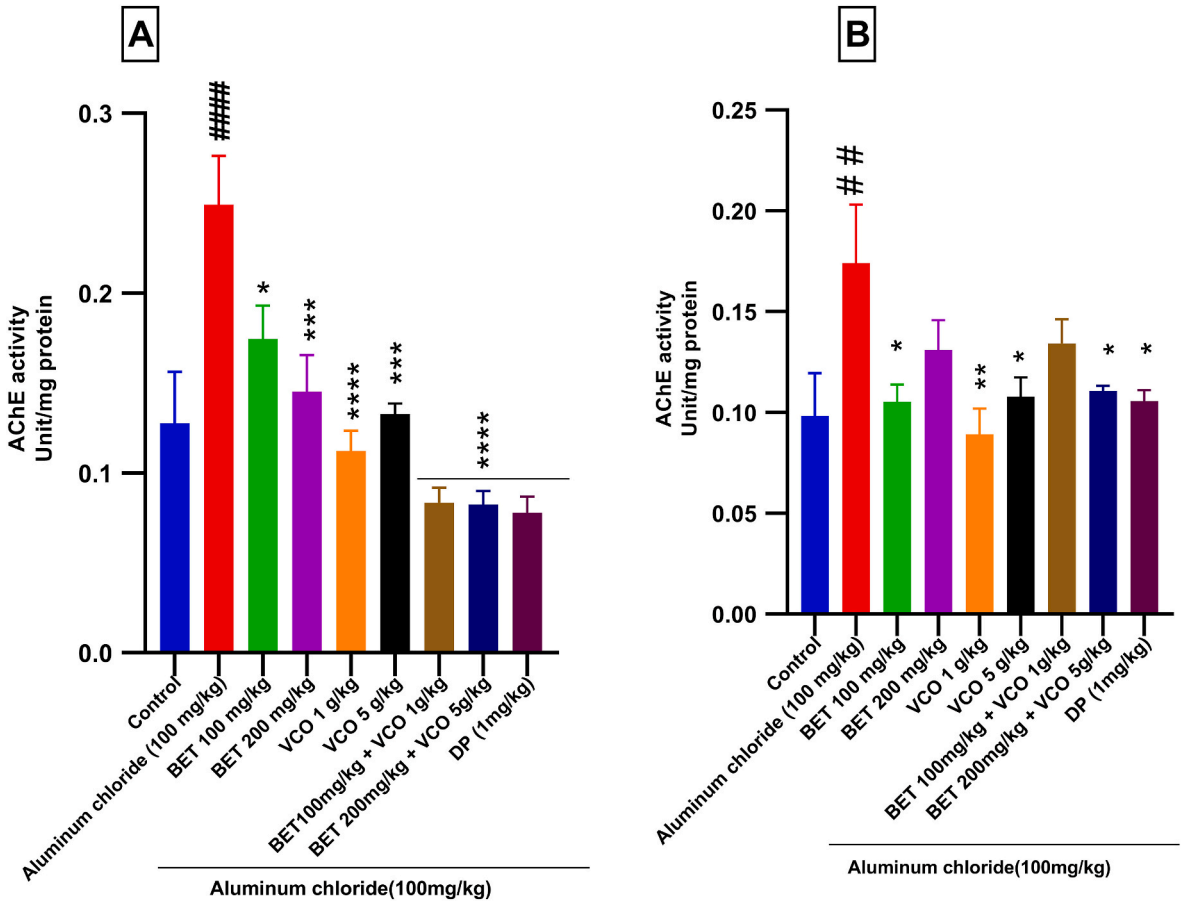

Fig. 3. Effect of BET and VCO on Acetylcholinesterase activity. A) Hippocampus B) Cortex. Data are expressed as mean ± SEM, $^{\#\#\#\#}p < 0.0001$, $^{\#\#}p < 0.01$ when compared with normal control, ****$p < 0.0001$ ***$p < 0.001$**$p < 0.01$,*$p < 0.05$ when compared to treatment group.

2.8. Histopathological analysis

A histopathological examination was performed on brain tissues preserved in 10 % neutral buffered formalin and embedded in paraffin sections. A microtome (Thermo Scientific, HM 325) was used to take the hippocampus and cortex area's thin transverse sections (3–5 μm thickness). The sections of brain tissues were stained using Hematoxylin, Eosin (H&E), and Congo red dye and analyzed under a digital microscope (Nikon, Eclipse, E 100) at a magnification of 400X—the examination aimed to assess the prevalence of neurodegeneration and amyloid beta accumulation in the brain.

3. Statistical analysis

All the results are expressed as Mean ± SEM. Behavioral parameters were assessed by two-way ANOVA followed by Tukey's post hoc test. In contrast, biochemical parameters were determined by one-way ANOVA followed by Dunnet's post hoc test, and the significance level was determined within and between groups ($P < 0.05$) using Graph Pad PrismV 8.0.

4. Result

4.1. Fatty acid profile of the virgin coconut oil

Virgin coconut oil was analyzed for fatty acid composition using GC-MS/FID. Primary ingredients were identified via mass fragmentation analysis. The oil's principal fatty acids are caproic, caprylic, lauric, and myristic (Supplementary file Fig. 1).

4.2. Acute toxicity study of the combination

Following the oral administration of BET at doses of 1000 and 2000 mg/kg and VCO at doses of 5 and 10 g/kg to a group of rats, no signs of toxicity or mortality were observed. These findings confirm that the combination is safe for use. Supporting data confirm that BET administration and VCO do not produce harmful consequences (Supplementary file Table 1).

4.3. Morris water maze (MWM)

We performed the MWM, and the Aluminium chloride induced rat markedly increased escape latency (EL) than the control group (Day 21 $^{\#}p < 0.01$ and Day 42 $^{\#\#\#\#}p < 0.0001$). BET, VCO, both the combinations and DP treatment significantly decreased in EL suggesting that all treatment could reverse the spatial memory deficit in AD rats (Day 21 *$p < 0.01$ and day42 ****$p < 0.0001$for 100 mg/kg; Day 21 n.s. and day42 $p < 0.0001$ for 200 mg/kg) (Day 42 ****$p < 0.0001$for for 1 g/kg) (day42 **$p < 0.01$for (100 mg/kg +1 g/kg); Day 21 **$p < 0.01$ and day 42 ****$p < 0.0001$ for (200 mg/kg + 5 g/kg) (Day 21 *$p < 0.05$ and day42 ****$p < 0.0001$). Based on our findings, the therapy has significantly enhanced lost spatial memory and learning abilities. These results suggested that the therapy may effectively improve cognitive function (Fig. 1).

4.4. Elevated plus maze (EPM)

We evaluated the EPM and observed that each rat's initial transfer latency (ITL) was generally constant and exhibited no significant change

Table 2
Effect of Combination on brain oxidative stress parameters in the cortex.

Group	MDA (nmol per mg protein)	GSH (μmol per mg protein)	SOD (U per mg protein)	CAT (nmol of H2O2 decomposed per min per mg protein)
Control	0.9996 ± 0.04	4.93 ± 0.51	0.092 ± 0.01	10.36 ± 1.84
Aluminum chloride (AlCl3)	2.181 ± 0.14$^{\#\#\#\#}$	1.352 ± 0.45$^{\#\#\#}$	0.045 ± 0.01$^{\#\#}$	2.062 ± 1.688$^{\#\#}$
AlCl3 + BET 100 mg/kg	1.512 ± 0.16**	2.711 ± 0.72	0.1 ± 0.01*	9.194 ± 1.919*
AlCl3 + BET 200 mg/kg	1.198 ± 0.16****	3.572 ± 0.63*	0.084 ± 0.008	9.998 ± 1.289*
AlCl3 + VCO 1 g/kg	0.6797 ± 0.08****	1.794 ± 0.40	0.065 ± 0.003	8.475 ± 2.581
AlCl3 + VCO 5 g/kg	0.9901 ± 0.09****	2.683 ± 0.39	0.076 ± 0.007	11.93 ± 1.478**
AlCl3 + BET 100 mg/kg and VCO 1 g/kg	1.18 ± 0.15****	2.909 ± 0.41	0.068 ± 0.004	8.589 ± 1.817
AlCl3 + + BET 200 mg/kg and VCO 5 g/kg	0.9255 ± 0.07****	4.056 ± 0.85**	0.087 ± 0.009*	10.37 ± 1.182**
AlCl3 + Donepezil HCl (1 mg/kg)	0.9353 ± 0.08****	1.676 ± 0.52	0.067 ± 0.001	10.27 ± 0.9914**

Data are expressed as mean ± S. E. M. (n = 6), $^{\#\#\#\#}$p < 0.0001, $^{\#\#\#}$p < 0.001, $^{\#\#}$p < 0.01 when compared with normal control, ****p < 0.0001, **p < 0.01, *p < 0.05 when compared with disease control group.

on day 20. Following training, BET (Day 21 n.s. and day 42 ***p < 0.001 for 100 mg/kg; Day 21 **p < 0.01 and day 42 ***p < 0.001 for 200 mg/kg) and VCO alone resulted in a considerable decrease in TL (Day 21 *p < 0.05 and day 42 ***p < 0.001 for 1 g/kg; Day 21 *p < 0.05 and day 42 **p < 0.01 for 5 g/kg). However, treatment with the combination (Day 21 ***p < 0.001 and day42 ****p < 0.0001 for (BET 100 mg/kg + VCO 1 g/kg); Day 21 **p < 0.01 and day42 ****p < 0.0001 for (BET 200 mg/kg + VCO 5 g/kg) and DP found to produce substantial decreases in TL (Day 21 *p < 0.05 and day 42 ****p < 0.0001). In contrast, the aluminum chloride treated group entered late in the closed compartment, as demonstrated by the increase in 2nd transfer latency at day 21 and 42 compared to ITL at day 20 (Day 21 $^{\#}$p < 0.05 and day 42 $^{\#\#\#}$p < 0.001). (Fig. 2A).

4.5. Passive avoidance (PA)

During the investigation of the PA test, we recorded the escape latency (EL) on day 20 and the retention latency (RL) on days 21 and 42. Each rat quickly enters the dark compartment on day 20. After receiving the shock, an increase in cognitive abilities was observed in the treatment group, as demonstrated by a significant increase in RL on days 21 and 42. In contrast, the aluminum chloride treated group showed impairment in cognitive abilities compared to the control group (Day 21 and Day 42 $^{\#\#\#\#}$p < 0.0001). The increase in RL was observed in BET (Day 21 and Day 42 ****p < 0.0001 for 100 mg/kg; Day 21 *p < 0.05 and Day 42 ****p < 0.0001 for 200 mg/kg), VCO (Day 21 and Day 42 ****p < 0.0001 for 1 g/kg; Day 42 **p < 0.01 for 5 g/kg). Furthermore, treatment with the combination (Day 42 ****p < 0.0001 for (BET 100 mg/kg + VCO 1 g/kg); day 42 **p < 0.01 for (BET 200 mg/kg + VCO 5 g/kg) and, DP significantly decreases the RL (Day 21 ***p < 0.001 and Day 42 ****p < 0.0001). The results indicated that the treatment group demonstrated an improvement in the learning capacity of the rodents (Fig. 2 B).

4.6. Acetylcholinesterase assay

After the behavioral test, we conducted biochemical studies using homogenates of the hippocampus and cortex portion of the brain. In the acetylcholinesterase assay of the hippocampus, the BET and VCO treatments significantly reduced AChE-specific activity. (*p < 0.05 for BET 100 mg/kg, and **p < 0.001 for BET 200 mg/kg; ****p < 0.0001 for VCO 1 g/kg and ***p < 0.001 for 5 g/kg). However, both combinations (BET 100 mg/kg + VCO 1 g/kg) (BET 200 mg/kg + VCO 5 g/kg) more efficiently lowered the acetylcholinesterase activity than the aluminum chloride group. (****p < 0.0001). (Fig. 3A).

In the cortex, the BET and VCO treatments significantly reduced AChE-specific activity. (*p < 0.05 for BET 100 mg/kg; **p < 0.01 for 1 g/kg; *p < 0.05 for 5 g/kg).However, a higher combination subsided the acetylcholinesterase activity more effectively than the aluminum chloride group in the cortex. (*p < 0.05). Based on the results, it can be inferred that both VCO and BET treatments contributed to the decrease in AChE activity in either region. However, combining these treatments was more effective in the hippocampus and cortex of the brain (Fig. 3B).

4.7. Brain oxidative parameters

A study was conducted aimed at the possible antioxidant effect of BET and VCO in particular brain regions.

4.7.1. Evaluation of hippocampus oxidative stress parameters

In the hippocampus, the one-way ANOVA indicated a substantial impact of therapy on the brain's oxidative state, SOD F (8, 45) = 3.356, P = 0.0043, CAT F (8, 45) = 2.108, P = 0.0547, the total content of reduced GSH F (8, 45) = 1.830, P = 0.0962, and higher levels of lipid peroxidation (MDA) F (8, 45) = 2.33, P < 0.0345. Table 1.

The specific activities of SOD were significantly lowered following aluminum chloride treatment ($^{\#\#}$p < 0.01) compared to the control. BET treatment increased SOD activity by decreasing aluminum chloride-induced oxidative stress. (**p < 0.01 for 100 and 200 mg/kg). The rest of the treatment exhibited non-significant differences.

The specific activities of GSH were considerably decreased following aluminum chloride treatment ($^{\#\#}$p < 0.01) compared to the control. Betanin (*p < 0.05 for 200 mg/kg), VCO (*p < 0.05 for 1 g/kg), and combination (*p < 0.05 for BET 200 mg/kg + VCO 5g) treatment increased GSH activity. However, standard treatment did not significantly differ from the aluminum chloride group.

Aluminum chloride treatment caused an increase in the specific activities of MDA ($^{\#\#}$p < 0.01). The combination treatment was more effective than the BET treatment alone in lowering MDA activity (*p < 0.05 for BET 100 mg/kg + VCO 1 g/kg and BET 200 mg/kg + VCO 5 g/kg). Furthermore, the VCO therapy was similarly efficacious (*p < 0.05 for 1 and 5 g/kg). However, standard and BET treatment did not significantly differ from the aluminum chloride group.

The specific activities of CAT were lowered due to aluminum chloride treatment ($^{\#\#}$p < 0.01) compared to the control. Betanin (*p < 0.05 for 100 and 200 mg/kg) and combination (*p < 0.05 for BET 100 mg/kg + VCO 1 g/kg) were able to significantly enhance CAT activity, while VCO at a dose of 1 g/kg treatment was more efficacious (*p < 0.01). However, standard treatment did not significantly differ from the aluminum chloride group (Table 1).

4.7.2. Evaluation of the cortical oxidative stress parameters

In the cortex, the one-way ANOVA indicated a significant impact of the therapy on the brain oxidative status, SOD F (8, 45) = 3.625, P = 0.0025, CAT F (8, 45) = 2.737, P = 0.0150, the total content of reduced GSH, F (8, 44) = 4.302, P = 0.0007, and raised levels of lipid peroxidation (MDA) F (8, 45) = 13.72, P < 0.0001.

The specific activities of SOD were significantly reduced following aluminum chloride treatment ($^{\#\#}$p < 0.01) compared to the control. BET (***p < 0.0001 for 100 mg/kg, *p < 0.05 for 200 mg/kg) and

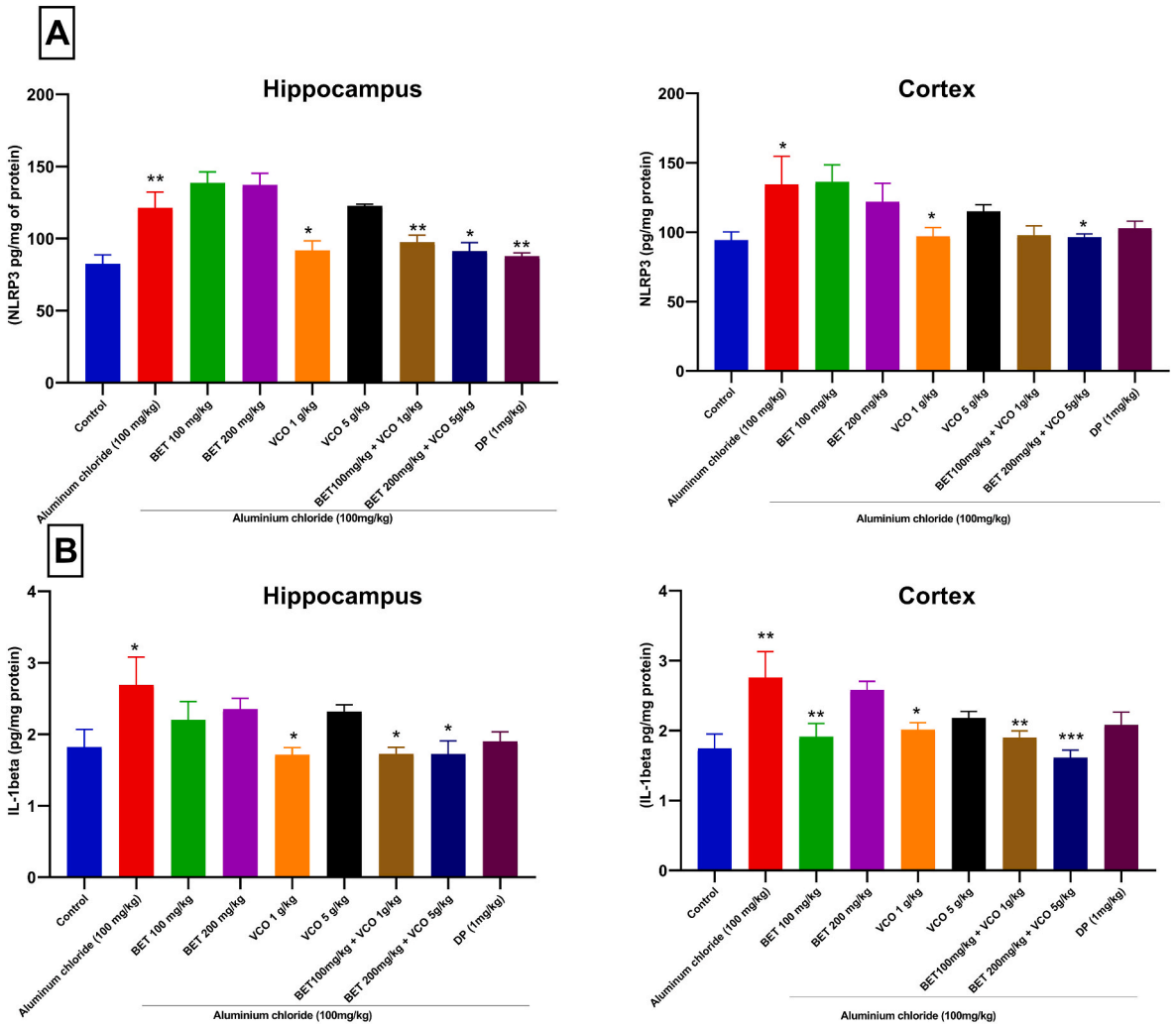

Fig. 4. Effect of BET and VCO on molecular markers. (A) NLRP3 (B) IL-1β Data are expressed as mean ± SEM, **p < 0.01, *p < 0.05when compared with normal control, ****p < 0.0001 ***p < 0.001**p < 0.01,*p < 0.05 when compared to treatment group.

combination (*p < 0.05 for BET 100 mg/kg + VCO 1 g/kg and BET 200 mg/kg + VCO 5g) treatment augmented SOD activity by subsiding oxidative stress. However, VCO and standard treatment did not significantly differ from the aluminum chloride group.

The specific activities of GSH were significantly reduced following aluminum chloride treatment ($^{\#\#\#}$p < 0.001) compared to the control. The combination was found more efficacious (**p < 0.01 for BET 200 mg/kg + VCO 5g) than BET treatment (*p < 0.05 for 200 mg/kg) in controlling oxidative stress. However, VCO and standard treatment did not significantly differ from the aluminum chloride group.

MDA activities were significantly elevated in the aluminum chloride group ($^{\#\#}$p < 0.01) compared to the control. All treatments reduced MDA activity more efficiently compared to the aluminum chloride group. BET (**p < 0.01 for 100 mg/kg, and ****p < 0.0001 200 mg/kg), VCO (****p < 0.0001 for 1 and 5 g/kg), combination (****p < 0.0001 for BET 100 mg/kg + VCO 1 g/kg and BET 200 mg/kg + VCO 5 g/kg), and DP (***p < 0.001).

The specific activities of CAT were significantly reduced following aluminum chloride treatment ($^{\#\#}$p < 0.01) compared to the control. BET (*p < 0.05 for 100 and 200 mg/kg) and VCO treatment improved activity by subsiding oxidative stress (**p < 0.01 for 5 g/kg). Both the combination (**p < 0.01 for BET 200 mg/kg + VCO 5 g/kg) and standard treatment with DP treatment improved CAT activity by reducing oxidative stress (**p < 0.01). According to our findings, treating BET or VCO alone can partially alleviate oxidative stress in both brain regions, which is consistent with the literature. However, when combined, BET and VCO showed a more significant impact and proved more effective in reducing oxidative stress (Table 2).

4.7.3. *Estimation of IL-1β level*

We further investigated IL-1β levels in both the hippocampus and cortex and observed that in the hippocampus, aluminum chloride treatment caused a substantial surge in IL-1β levels in a rat's brain ($^{\#}$p < 0.05) compared to the control group. BET co-administration did not reduce the level of IL-1β. However, treatment with VCO (1 g/kg) (*p < 0.05) significantly decreased the level of IL-1β as compared to aluminum chloride-treated animals. Moreover, treatment with a combination significantly reduced its level (*p < 0.05 for BET 100 mg/kg + VCO 1 g/kg and BET 200 mg/kg + VCO 5 g/kg).

In the cortex, treatment with the combination was found more effective in controlling IL-1β levels (**p < 0.01 for BET 100 mg/kg + VCO 1 g/kg and ***p < 0.001 for BET 200 mg/kg + VCO 5 g/kg). Aluminum chloride caused a substantial increase in IL-1β level ($^{\#\#}$p < 0.001) in contrast to the control group. BET at a dose of 100 mg/kg (**p < 0.01) and VCO (1 g/kg) (*p < 0.05) significantly decrease the level of IL-1β (Fig. 4B). The study demonstrated that the combined therapy reduced the amount of IL-1β in the cortex and hippocampus, whereas each therapy alone had a limited impact on the rat brain.

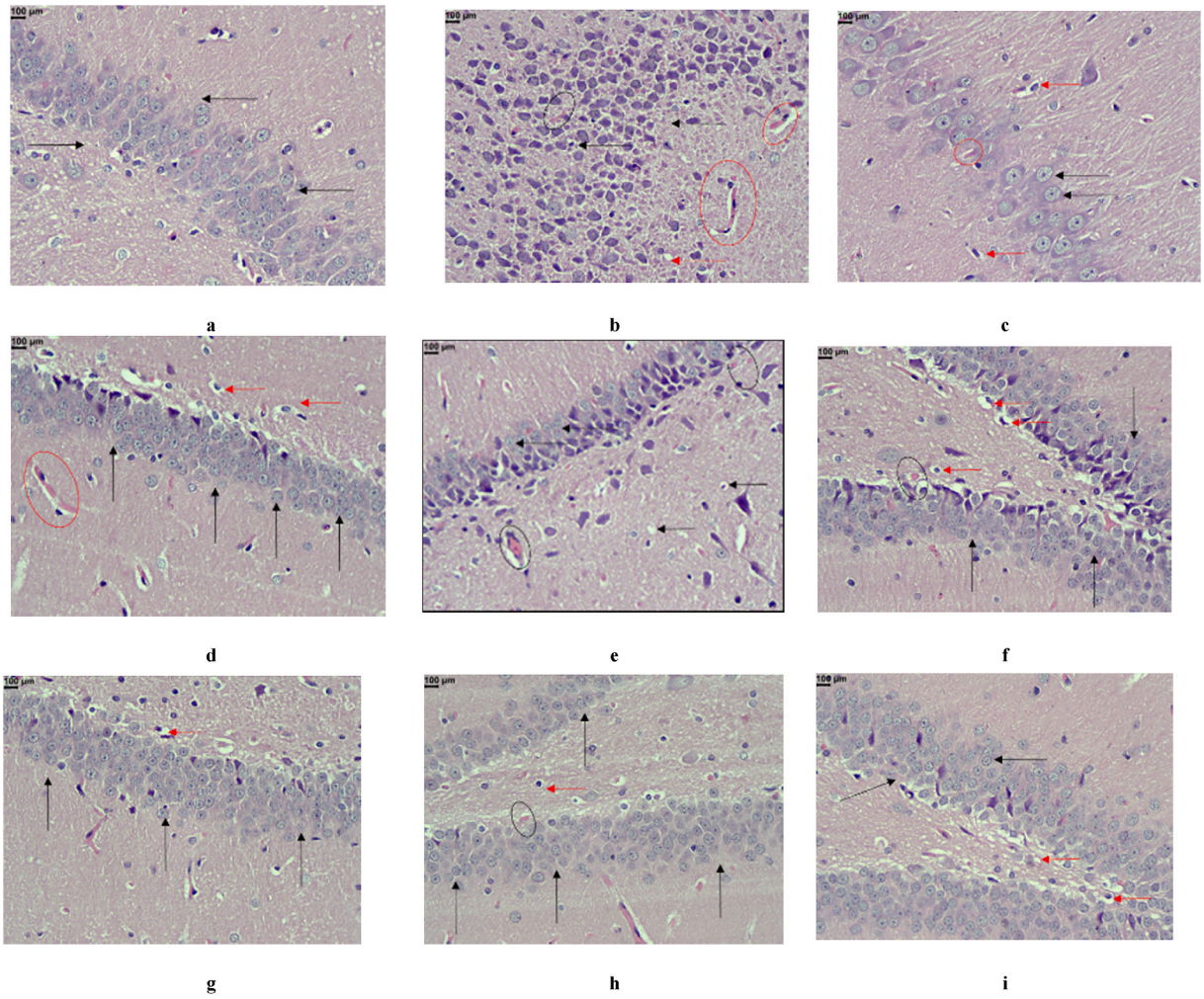

Fig. 5a. Representative light microphotographs H and E stained hippocampus a) Normal histological characteristics, including normal neurons and normal pyramidal cell layer thickness of the CA3 area (black arrow) **b)** Pyramidal cell layer thickness significantly reduced, and there were more apoptotic neurons, dystrophic changes, hyperchromatic, and abnormal Nissl granule distributions (black arrows), vascular/capillary engorgement (red circle), Hirano bodies (black circle), and degenerated and vacuolated neurocytes (Red arrow) **c)** Decreased thickness of pyramidal cell layer, degenerated, vacuolated neurons (red arrow), and vascular/capillary engorgement (red circle). **d)** Normal histological features (black arrows) with a small number of degenerated and vacuolated neurons (red arrow), and vascular/capillary engorgement (red circle).**e)** vacuolated neurons (red arrow), and vascular/capillary engorgement (red circle).**f)** A small number of degenerated and vacuolated neurons (red arrow), and vascular/capillary engorgement (red circle) with preserved hippocampal cell layers g) Normal histological features, with normal neurons (black arrows) with a small number of degenerated and vacuolated neurons (red arrow) h) Normal thickness of the pyramidal cell layer of the CA3 region, with normal neurons (black arrows) with a small number of degenerated and vacuolated neurons (red arrow) **i)** A small number of apoptotic neurons (red arrow). The granular area displays signs of cellular recovery with intact hippocampus cell layers. **(H and E (400X) (Scale bar = 100 μm)**.

4.7.4. Estimation of NLRP3 level

We assessed the levels of NLRP3 in the cortex and hippocampus. Aluminum chloride treatment triggered a noteworthy upsurge in NLRP3 level in the hippocampus of a rat ($^{\#}p < 0.01$) in contrast to the control group. The combination ($^{*}p < 0.05$ for BET 200 mg/kg + VCO 5 g/kg and $^{**}p < 0.01$ for BET 100 mg/kg + VCO 1 g/kg), VCO (1 g/kg) ($^{*}p < 0.05$) and DP significantly decreases the level of NLRP3 ($^{**}p < 0.01$ 2 mg/kg). However, BET co-administration did not significantly reduce it.

In the cortex region, aluminum chloride treatment significantly increased NLRP3 level in a rat's brain ($^{\#}p < 0.05$) compared to the control group. The combination ($^{*}p < 0.05$ for BET 200 mg/kg + VCO 5 g/kg) and VCO (1 g/kg) was found equally effective in controlling the level of NLRP3 ($^{*}p < 0.05$). However, BET and DP did not significantly reduce it. It was found that using BET alone did not provide any significant advantages. However, a more notable result was observed when combined with VCO (Fig. 4A).

4.8. Histopathological analysis

4.8.1. Hematoxylin and eosin

After the biochemical studies, we conducted histological analysis of the hippocampus and cortical area using hematoxylin and eosin staining. The aluminum chloride-treated animals demonstrated distinct histological alterations in neuronal degeneration and necrosis in the hippocampus and cortex. We observed normal brain parenchyma and neurons in the control group. Furthermore, no pathologically significant lesions were observed in this group. The treatment group (BET 100, 200 mg/kg, and VCO 1 g/kg and 5 g/kg) lessened the severity of hippocampal and cortex neuronal degeneration and necrosis. A combination (BET 100 mg/kg + VCO 1 g/kg and BET 200 mg/kg + VCO 5 g/kg) and DP had a substantial ameliorating impact compared to the other treatment groups. BET or VCO alone can slightly reduce the damage caused by aluminum chloride, but when used in combination, they have a significant impact on recovering the brain's structure (Fig. 5).

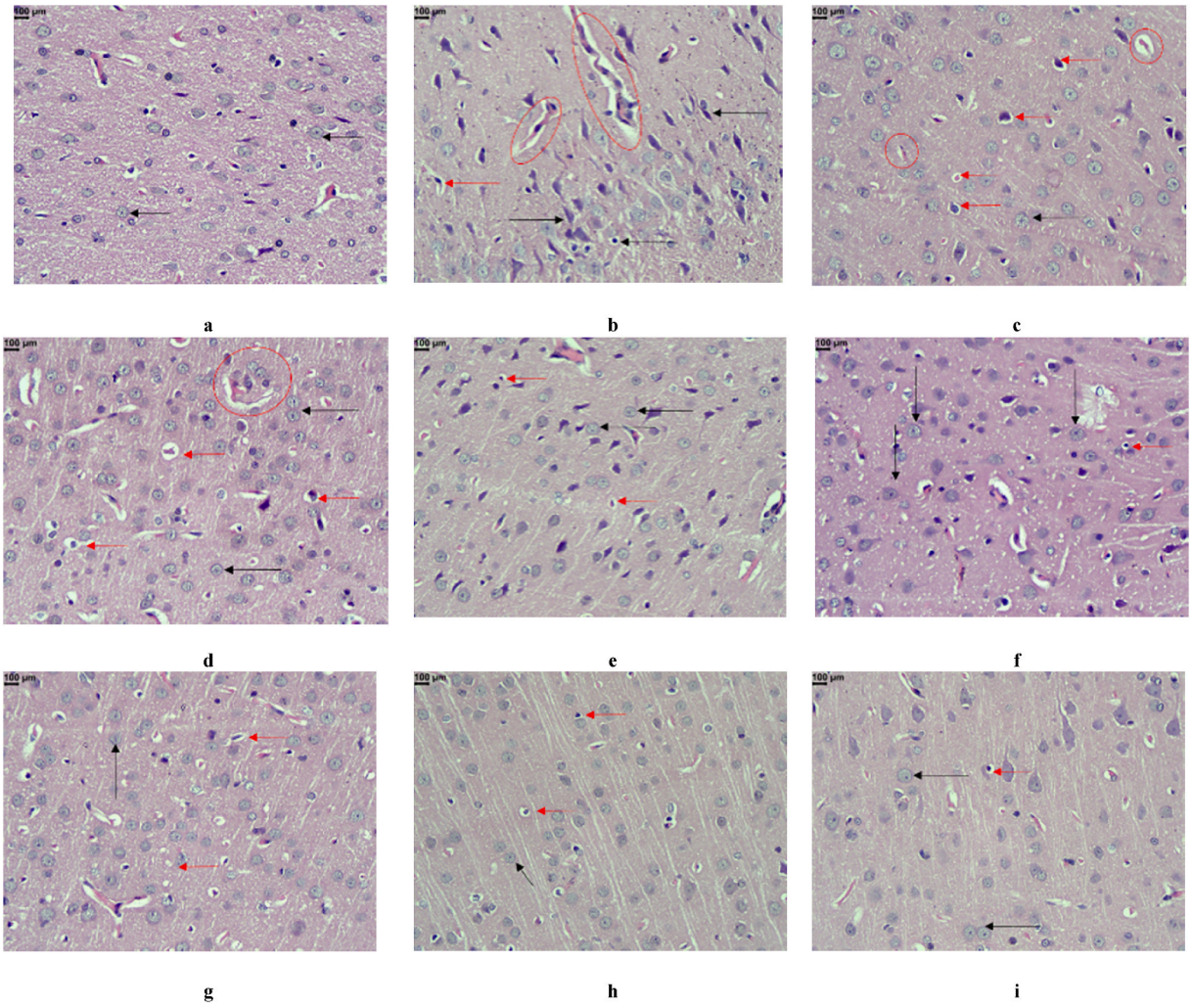

Fig. 5b. Representative light microphotographs H and E stained cortex tissue of rats: a) Normal neurons have Nissl granules distributed around the periphery and a core big vesicular nucleus with one or more nucleoli b) Dystrophic neurons with abnormal Nissl granule distribution and hyperchromatic morphology (black arrows), with dilated blood vessel (red circle), degenerated, and vacuolated neurocytes (red arrow) c), d) normal neurons (black arrow) degenerated neurons (red arrows) vascular/capillary engorgement (red circle) e),f) Normal neurons (black arrow) degenerated neurons (red arrows) vascular/capillary engorgement (red circle) g), h), and i) normal neurons (black arrow) few degenerated neurons (red arrows), the granular layer demonstrates cellular recovery. **(H and E (400X) (Scale bar = 100 µm).**

4.8.2. Congo red stain

The accumulation of amyloid-beta plaques accompanies altered glucose metabolism and loss of synapses, leading to a gradual decline in cognitive function. Therefore, the hippocampus and cortex staining with congo red dye were used to detect the presence of these plaques. The aluminum chloride group showed amyloid-beta plaque, neuronal degeneration, nuclear pyknosis, and necrosis in the cortex and CA3 region of the hippocampus of the brain when compared with a control group. The control group showed normal cerebral parenchyma and neurons in the cortex and CA3 region of the hippocampus. BET (100, 200 mg/kg) and VCO (1 g/kg and 5 g/kg) treatment reduced the severity of neuronal degeneration, nuclear pyknosis, amyloid-beta plaque formation, and necrosis in the CA3 region of the hippocampus. A combination of the test treatment (BET 100 mg/kg + VCO 1 g/kg and BET 200 mg/kg + VCO 5 g/kg) and group DP showed a significant reduction in the incidence and severity of these changes. Based on the congo stain results, it appears that BET or VCO partially reduces neurodegeneration and amyloid beta plaque formation in either of the regions, while their combination protects the brain in both the hippocampus and cortex (Fig. 6).

5. Discussion

The NLRP3 inflammasome is formed during the etiology of AD. The lysosomal damage theory, reactive oxygen species hypothesis, and mitochondrial DNA theory are all proposed explanations for NLRP3 inflammasome activation. This activation increases the incidence of AD by generating IL-1β, IL-18, and other cytokines and subsequently influencing the accumulation of Aβ and tau proteins.[28]

Alteration of glucose metabolism is a prominent hallmark of AD, and it occurs before the symptomatic onset of the disease. Ketone bodies can be used as an alternative fuel without glucose. VCO comprises medium-chain triglycerides (MCT) that are converted to MCFA by the enzyme lipase. Ketone bodies are formed when MCFAs are metabolized. Ketone bodies have direct and indirect signaling properties that control neuroinflammation.[29] In our study, we observed the presence of the following MCTs: caproic acid (C6), caprylic acid (C8), lauric acid (C12), and myristic acid (C14) in VCO by Gas chromatography-mass spectrometry (GCMS) analysis method. MCTs might be responsible for decreasing neuroinflammation in aluminum chloride-induced rats.

Chemical toxins such as metals can affect brain function and cause changes in behavior, thinking, or emotion.[30] In the current study,

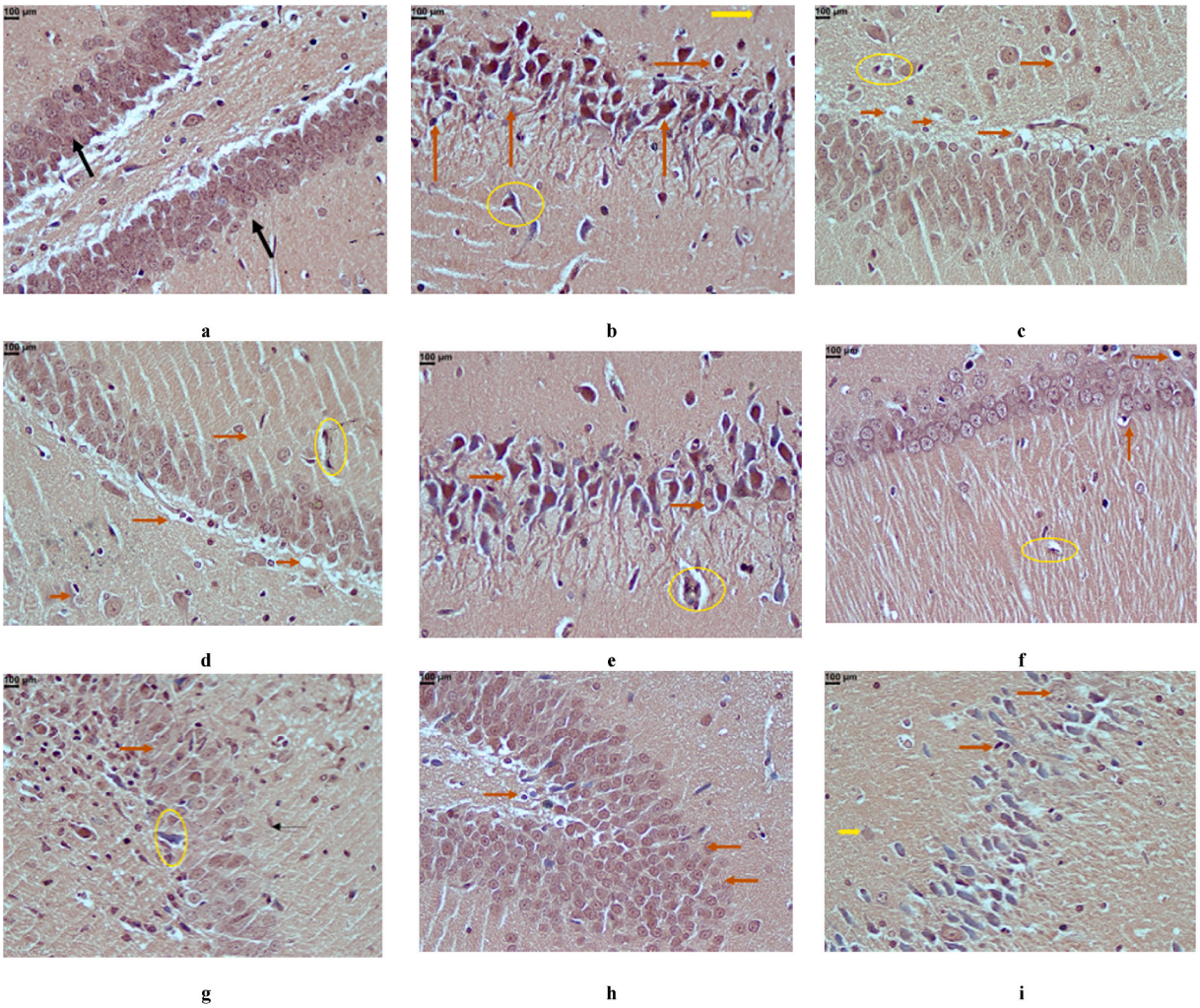

Fig. 6a. Representative light microphotographs of Congo red stained hippocampus of rat a) Normal histological features with normal thickness of the pyramidal cell layer of the CA3 region, with normal neurons (black arrows) b) Decreased thickness of pyramidal cell layer in the CA3 region, with increased apoptotic neurons (arrows) with dilated blood vessel (circle), and degenerated and vacuolated neurocytes. Amyloid plaque (Yellow arrow) c) Normal thickness of the pyramidal cell layer with normal neurons (black arrows) with a small number of apoptotic neurons (arrow), Granulovascular degeneration (circle) d) Normal thickness, with normal neurons (black arrows) with a small number of apoptotic neurons (arrow). Also, observed granulovascular degeneration (circle) e) A small number of apoptotic neurons (arrow), the granulovascular degeneration, the sign of early neuronal degeneration. Amyloid plaque (Yellow arrow) f) Normal thickness with normal neurons (black arrows) with a small number of apoptotic neurons (arrow), the granulovascular degeneration g) normal neurons (black arrows) with some apoptotic neurons (arrow), the granulovascular degeneration in few neurons h) Preserved hippocampal cell layers, with normal neurons (arrows) i) Normal thickness of the pyramidal cell layer with normal neurons (arrows) with a small number of apoptotic neurons (arrow), the granulovascular degeneration in few neurons. Amyloid plaque (yellow arrow). **Congo red stained hippocampus and cortex tissue (400X) (Scale bars = 100 μm).**

treatment with $AlCl_3$ for 42 days reduced step-through latencies in the PA test, increased transfer latency in the EPM, and increased escape latency in the MWM test. It indicates the cognitive deficit in animals. The MWM approach was designed to evaluate the spatial memory in animals to find a hidden platform in the pool of water using visual clues placed in each quadrant of the water maze.[31] Betanin, VCO, and combination-treated animals reached the escape platform earlier than the AlCl3 group. PA is a fear-motivated test that measures pre and post-shock latencies to evaluate short and long-term memory. Post-shock latency was longer in groups treated with BET, VCO, and combination than with the aluminum chloride group, suggesting that rats' recognition memory had improved. The EPM test determines spatial learning and memory by evaluating initial transfer latency (ITL) and retention transfer latency (RTL). BET, VCO alone, and combination treatments reduced RTL after ITL determination, indicating that rats' recognition memory had significantly improved compared to the aluminum chloride group.

Increased AChE activity observed in aluminum-treated rats is related to the cholinergic deficit theory of cognitive impairment.[32] Aluminum may increase AChE activity by creating an allosteric interaction between the Al^{+3} and anionic regions of the acetylcholinesterase enzyme that results in a change in the secondary structure of AChE in the brain, which then contributes to acetylcholine hydrolysis.[33] In this study, we observed that AChE activity was higher in the aluminum chloride treatment group compared to control rats. AChE activity was reduced after treatment with a combination of BET and VCO (BET 200 mg/kg + VCO 5 g/kg), equal to the DP group. However, we did not observe the activity in the cortex.

One of the most significant biomarkers of oxidative stress is lipid peroxidation. Aluminum has been shown to activate and promote lipid peroxidation when iron is in the brain.[34] Increased oxidative stress causes redox reactions that inhibit different antioxidative enzymes such as catalase, superoxide dismutase, and reduced glutathione. All of which are important in preventing free radical damage. Chronic $AlCl_3$ administration has been shown to enhance brain MDA while decreasing SOD, CAT, and GSH levels in various brain areas that back up our results.[19,35]

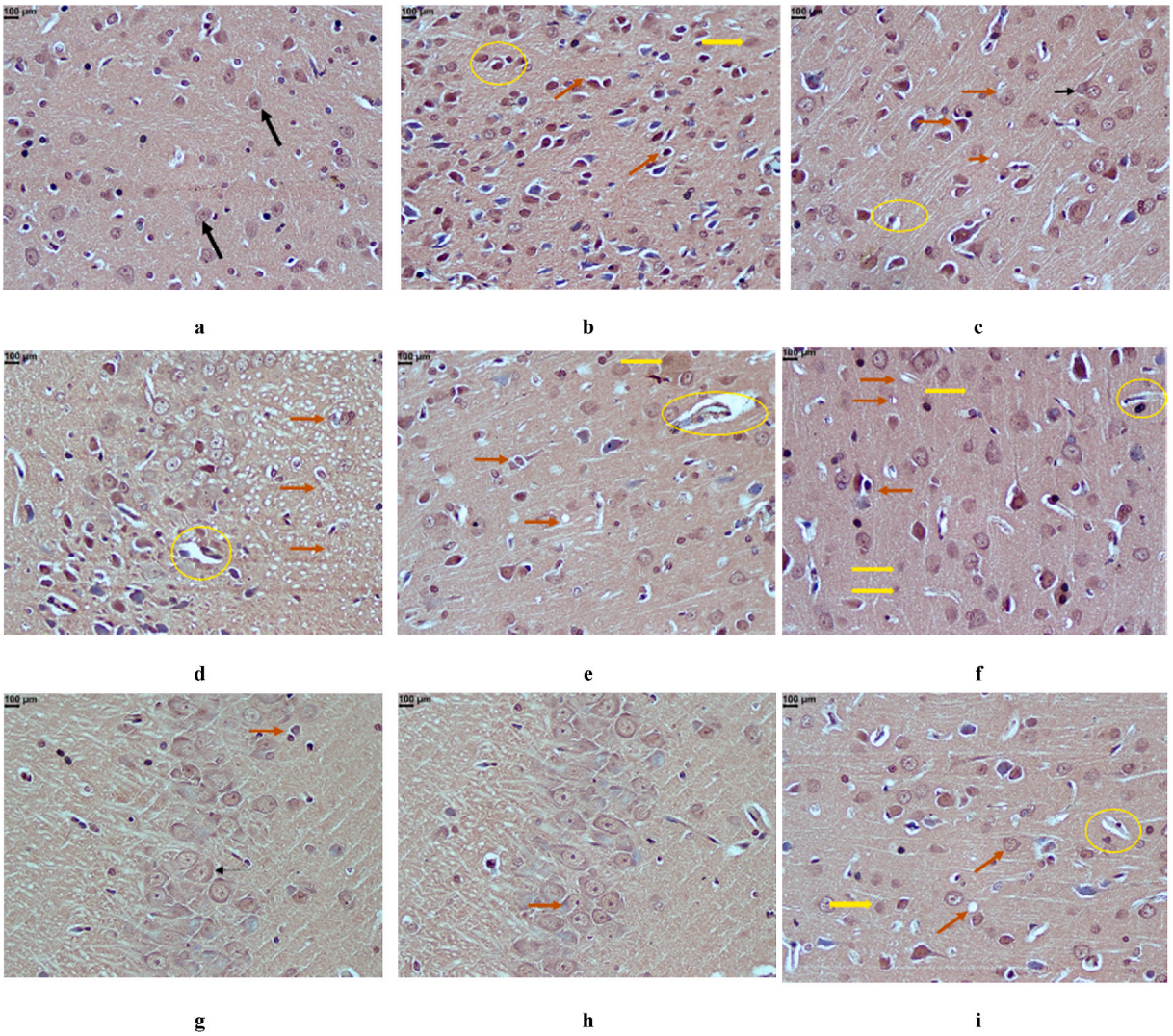

Fig. 6b. Representative light microphotographs of Congo red stained hippocampus and cortex tissue of rat **a)** normal histological features with stratified layers. Neurons with a core large vesicular nucleus that contains one or more nucleoli and distribution of Nissl granules on the periphery **b)** Dystrophic, hyperchromatic, irregularly scattered Nissl granules (arrows), with dilated blood vessel (circle), and degenerate and several vacuolated neurocytes (arrow).Amyloid plaque (Yellow arrow).**c)** A small number of apoptotic neurons, an early sign of neurodegeneration (arrows).**d)** Degenerate and number of vacuolated neurocytes (arrow), dilated blood vessels (circle) **e), f)** normal neurons (black arrow), a small number of neurons with apoptotic, irregular, vacuolated neurocytes (arrows), dilated blood vessels (circle) Amyloid plaque (Yellow arrow) **g)** Few apoptotic neurons (arrow) h) normal neurons with signs of cell recovery (arrow) i) Normal histological features with stratified layers (arrow), dilated blood vessels (circle). **Congo red stained hippocampus and cortex tissue (400X) (Scale bars = 100 μm).**

VCO supplementation and betalains were discovered to have antioxidant effects by increasing the enzymatic and non-enzymatic antioxidants separately.[36,37]

In our study, the combination of both (BET 100 mg/kg + VCO 1 g/kg and BET 200 mg/kg + VCO 5 g/kg) provides a wide range of protection against oxidative stress. It might be due to MCT and betalains in VCO and BET, respectively. MCT is found in VCO. It is efficient at inducing ketosis via MCFA when consumed. MCFA is absorbed at the same rate as glucose and metabolizes quickly.[38] Ketosis can potentially lower reactive oxygen species (ROS) and alter inflammatory pathways.[39] Ketone-inducing therapy has been demonstrated to influence mitochondrial function.[40] Thus, VCO directly controls ROS generation at the mitochondrial level. However, VCO must be administered in greater dosages to evoke a ketogenic response. As a result, combining VCO with additional antioxidants is advised.[41] In one of the studies, the combination of VCO plus a Mediterranean diet increased episodic memory, temporal orientation, and semantic memory.[42]In this study, we combined BET because it inhibits ROS production in AlCl3-treated rats, allowing us to limit the VCO dosage successfully.

The NLRP3 inflammasome forms due to a wide variety of DAMPs. Caspase-1, as an inflammasome regulatory protein, may convert inactive IL-1β and IL-18 precursor proteins into active IL-1β and IL-18, respectively. They play several non-specific inflammatory functions.[43] TNF-α, IL-1β, and IL-6 are several downstream pro-inflammatory mediators stimulated by IL-1β.[44] Thus, the activation or inhibition of the NLRP3 inflammasome alters the neuroinflammation process, which may influence the generation and release of IL-1β.[45] Also, The inflammasome NLRP3 connects Aβ plaques and neurofibrillary tangles.[28] The NLRP3 protein and the pro-inflammatory mediator IL-1β are pivotal in Alzheimer's disease pathogenesis. Because an aluminum deposition can cause neuroinflammation,[46] we observed that the AlCl3 group had higher levels of NLRP3 and IL-1β in our investigation. However, treatment with BET and VCO alone did not significantly lower levels compared to the $AlCl_3$ group in the hippocampus and cortex. On the other hand, the combination groups (BET 100 mg/kg + VCO 1 g/kg and BET 200 mg/kg + VCO 5 g/kg) have been observed to decrease NLRP3 and IL-1β levels in both parts of the brain. It suggests that the combination was effective in lowering neuroinflammation not only in the

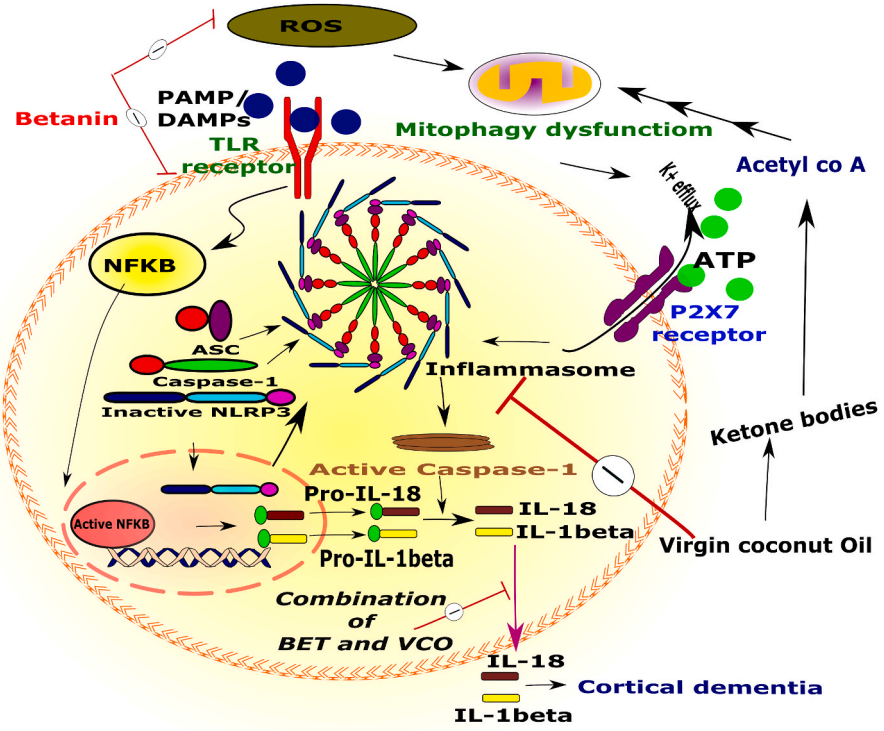

Fig. 7. BET combined with VCO prevents neuroinflammation by inhibiting NLRP3 inflammasome activation in microglia.

hippocampus but also in the cortex.

Excessive Al accumulation results in a hippocampus inflammatory lesion (HIL) in CA1 and CA3 portions.[47] In rats, $AlCl_3$ treatment caused substantial hippocampus damage, especially in the CA and DG areas.[48] This experiment showed marked neurodegeneration in hematoxylin and eosin-stained brain tissue from the disease control group. The combination group (BET 100 mg/kg + VCO 1 g/kg and BET 200 mg/kg + VCO 5 g/kg) reduced the severity of neuronal degeneration and necrosis in the hippocampus and cortex detected by the H and E staining method.

Congo red dye was used to examine the accumulation of Aβ plaques. The production and accumulation of amyloid beta-protein are believed to be caused by a buildup of aluminum in the brain.[49] An amyloid-beta plaque and neurodegeneration were observed in the cortex and CA3 region of the hippocampus. On the other hand, combination therapy (BET 100 mg/kg + VCO 1 g/kg and BET 200 mg/kg + VCO 5 g/kg) reduced the formation of Aβ plaques in the hippocampus and cortex.

The neuropathological changes in AD first manifest in the entorhinal cortex and hippocampal regions. Later, they move to other temporal, parietal, and lastly, frontal association cortices.[50] We observed that the individual drug and the combination were influential in the hippocampus, but the individual drug had less or no impact on the cortex. A higher combination was found to be very effective in both brain regions. However, more extensive research should be conducted to understand combinations' effects better. Furthermore, we must create a low-cost dosage form that can be translated into humans (Fig. 7).

6. Conclusion

It can be concluded that the combination's beneficial effect on cognitive improvement is related to its antioxidant and anti-inflammatory capabilities and can decrease AChE activity, NLRP3, and IL-1β levels in an $AlCl_3$-induced AD rat model not only in the hippocampus but also in the cortex. This study provides evidence to investigate a new therapy option for AD via modulating the NLRP3 inflammasome pathway.

Funding details

None.

Declaration of competing interest

The authors report no declarations of interest.

Acknowledgments

I would like to thank SPPSPTM, SVKM's NMIMS University, Mumbai, for providing the animal research facility and support towards the completion of the project.

Appendix A. Supplementary data

Supplementary data to this article can be found online at https://doi.org/10.1016/j.jtcme.2023.11.001.

References

1. Zahid A, Li B, Kombe AJK, Jin T, Tao J. Pharmacological inhibitors of the nlrp3 inflammasome. *Front Immunol.* 2019;10(OCT):1–10. https://doi.org/10.3389/fimmu.2019.02538.
2. Rosa JM, Camargo A, Wolin IAV, Kaster MP, Rodrigues ALS. Physical exercise prevents amyloid β1−40-induced disturbances in NLRP3 inflammasome pathway in the hippocampus of mice. *Metab Brain Dis.* 2021;36(2):351–359. https://doi.org/10.1007/s11011-020-00646-8.
3. Jo EK, Kim JK, Shin DM, Sasakawa C. Molecular mechanisms regulating NLRP3 inflammasome activation. *Cell Mol Immunol.* 2016;13(2):148–159. https://doi.org/10.1038/cmi.2015.95.
4. White CS, Lawrence CB, Brough D, Rivers-Auty J. Inflammasomes as therapeutic targets for Alzheimer's disease. *Brain Pathol.* 2017;27(2):223–234. https://doi.org/10.1111/bpa.12478.
5. Lou G, Palikaras K, Lautrup S, Scheibye-Knudsen M, Tavernarakis N, Fang EF. Mitophagy and neuroprotection. *Trends Mol Med.* 2020;26(1):8–20. https://doi.org/10.1016/j.molmed.2019.07.002.
6. Han X, Xu T, Fang Q, et al. Quercetin hinders microglial activation to alleviate neurotoxicity via the interplay between NLRP3 inflammasome and mitophagy. *Redox Biol.* 2021;44, 102010. https://doi.org/10.1016/j.redox.2021.102010.

7. Biasizzo M, Kopitar-Jerala N. Interplay between NLRP3 inflammasome and autophagy. *Front Immunol*. 2020;11(October):1–14. https://doi.org/10.3389/fimmu.2020.591803.
8. Avgerinos KI, Egan JM, Mattson MP, Kapogiannis D. Medium Chain Triglycerides induce mild ketosis and may improve cognition in Alzheimer's disease. A systematic review and meta-analysis of human studies. *Ageing Res Rev*. 2020;58, 101001. https://doi.org/10.1016/j.arr.2019.101001.
9. Polturak G, Aharoni A. "La Vie en Rose": biosynthesis, Sources, and Applications of Betalain Pigments. *Mol Plant*. 2018;11(1):7–22. https://doi.org/10.1016/j.molp.2017.10.008.
10. Kaur G, Thawkar B, Dubey S, Jadhav P. Pharmacological potentials of betalains. *J Compl Integr Med*. 2018;15(3):1–9. https://doi.org/10.1515/jcim-2017-0063.
11. Lu X, Wang Y, Zhang Z. Radioprotective activity of betalains from red beets in mice exposed to gamma irradiation. *Eur J Pharmacol*. 2009;615(1-3):223–227. https://doi.org/10.1016/j.ejphar.2009.04.064.
12. Ramesh SV, Krishnan V, Praveen S, Hebbar KB. Dietary prospects of coconut oil for the prevention and treatment of Alzheimer's disease (AD): a review of recent evidences. *Trends Food Sci Technol*. 2021;112:201–211. https://doi.org/10.1016/j.tifs.2021.03.046.
13. Robinson SA, O'Brien MW, Grandy SA, Heinze-Milne S, Kimmerly DS. Short-term supplement of virgin coconut oil improves endothelial-dependent dilation but not exercise-mediated hyperemia in young adults. *Nutr Res*. 2019;67:17–26. https://doi.org/10.1016/j.nutres.2019.03.016.
14. Lee EJ, Oh H, Kang BG, et al. Lipid-lowering effects of medium-chain triglyceride-enriched coconut oil in combination with licorice extracts in experimental hyperlipidemic mice. *J Agric Food Chem*. 2018;66(40):10447–10457. https://doi.org/10.1021/acs.jafc.8b04080.
15. Mirzaei F, Khazaei M, Komaki A, Amiri I, Jalili C. Virgin coconut oil (VCO) by normalizing NLRP3 inflammasome showed potential neuroprotective effects in Amyloid-β induced toxicity and high-fat diet fed rat. *Food Chem Toxicol*. 2018;118 (April):68–83. https://doi.org/10.1016/j.fct.2018.04.064.
16. Cummings JL, Tong G, Ballard C. Treatment combinations for alzheimer's disease: current and future pharmacotherapy options. *J Alzheim Dis*. 2019;67(3):779–794. https://doi.org/10.3233/JAD-180766.
17. *OECD. Test No. 423: Acute Oral Toxicity - Acute Toxic Class Method*. OECD Publishing; 2002. https://doi.org/10.1787/9789264071001-en.
18. Ahmad Rather M, Justin-Thenmozhi A, Manivasagam T, Saravanababu C, Guillemin GJ, Essa MM. Asiatic acid attenuated aluminum chloride-induced tau pathology, oxidative stress and apoptosis via AKT/GSK-3β signaling pathway in wistar rats. *Neurotox Res*. 2019;35(4):955–968. https://doi.org/10.1007/s12640-019-9999-2.
19. Auti ST, Kulkarni YA. Neuroprotective effect of cardamom oil against aluminum induced neurotoxicity in rats. *Front Neurol*. 2019;10(April):1–17. https://doi.org/10.3389/fneur.2019.00399.
20. Singh NA, Bhardwaj V, Ravi C, Ramesh N, Mandal AKA, Khan ZA. EGCG nanoparticles attenuate aluminum chloride induced neurobehavioral deficits, beta amyloid and tau pathology in a rat model of Alzheimer's disease. *Front Aging Neurosci*. 2018;10(AUG). https://doi.org/10.3389/fnagi.2018.00244.
21. Sharma AC, Kulkarni SK. Evaluation of learning and memory mechanisms employing elevated plus-maze in rats and mice. *Prog Neuro-Psychopharmacol Biol Psychiatry*. 1992;16(1):117–125. https://doi.org/10.1016/0278-5846(92)90014-6.
22. Barkur RR, Bairy LK. Evaluation of passive avoidance learning and spatial memory in rats exposed to low levels of lead during specific periods of early brain development. *Int J Occup Med Environ Health*. 2015;28(3):533–544. https://doi.org/10.13075/ijomeh.1896.00283.
23. Ellman GL, Courtney KD, Andres V, Feather-Stone RM. A new and rapid colorimetric determination of acetylcholinesterase activity. *Biochem Pharmacol*. 1961;7:88–95. http://www.ncbi.nlm.nih.gov/pubmed/13726518.
24. Ohkawa H, Ohishi N, Yagi K. Assay for lipid peroxides in animal tissues by thiobarbituric acid reaction. *Anal Biochem*. 1979;95(2):351–358. https://doi.org/10.1016/0003-2697(79)90738-3.
25. Ellman GL. Tissue sulfhydryl groups. *Arch Biochem Biophys*. 1959;82(1):70–77. https://doi.org/10.1016/0003-9861(59)90090-6.
26. Lück H. Catalase. In: *Methods of Enzymatic Analysis*. Elsevier; 1965:885–894. https://doi.org/10.1016/B978-0-12-395630-9.50158-4.
27. Paoletti F, Aldinucci D, Mocali A, Caparrini A. A sensitive spectrophotometric method for the determination of superoxide dismutase activity in tissue extracts. *Anal Biochem*. 1986;154(2):536–541. https://doi.org/10.1016/0003-2697(86)90026-6.
28. Zhang Y, Dong Z, Song W. NLRP3 inflammasome as a novel therapeutic target for Alzheimer's disease. *Signal Transduct Target Ther 2020 51*. 2020;5(1):1–2. https://doi.org/10.1038/s41392-020-0145-7.
29. Chatterjee P, Fernando M, Fernando B, et al. Potential of coconut oil and medium chain triglycerides in the prevention and treatment of Alzheimer's disease. *Mech Ageing Dev*. 2020;186(January), 111209. https://doi.org/10.1016/j.mad.2020.111209.
30. Needleman HL. Behavioral toxicology. *Environ Health Perspect*. 1995;103(SUPPL. 6):77–79. https://doi.org/10.1289/ehp.95103s677.
31. Morris RGM, Garrud P, Rawlins JNP, O'Keefe J. Place navigation impaired in rats with hippocampal lesions. *Nature*. 1982;297(5868):681–683. https://doi.org/10.1038/297681a0.
32. Martorana A, Esposito Z, Koch G. Beyond the cholinergic hypothesis: do current drugs work in alzheimer's disease? *CNS Neurosci Ther*. 2010;16(4):235. https://doi.org/10.1111/J.1755-5949.2010.00175.X.
33. Kaizer RR, Corrêa MC, Spanevello RM, et al. Acetylcholinesterase activation and enhanced lipid peroxidation after long-term exposure to low levels of aluminum on different mouse brain regions. *J Inorg Biochem*. 2005;99(9):1865–1870. https://doi.org/10.1016/j.jinorgbio.2005.06.015. SPEC. ISS.
34. Sakamoto T, Ogasawara Y, Ishii K, Takahashi H, Tanabe S. Accumulation of aluminum in ferritin isolated from rat brain. *Neurosci Lett*. 2004;366(3):264–267. https://doi.org/10.1016/j.neulet.2004.05.045.
35. Mohamed EA, Ahmed HI, Zaky HS, Badr AM. Sesame oil mitigates memory impairment, oxidative stress, and neurodegeneration in a rat model of Alzheimer's disease. A pivotal role of NF-κB/p38MAPK/BDNF/PPAR-γ pathways. *J Ethnopharmacol*. 2021;267, 113468. https://doi.org/10.1016/j.jep.2020.113468.
36. Shunan D, Yu M, Guan H, Zhou Y. Neuroprotective effect of Betalain against AlCl3-induced Alzheimer's disease in Sprague Dawley Rats via putative modulation of oxidative stress and nuclear factor kappa B (NF-κB) signaling pathway. *Biomed Pharmacother*. 2021;137(January), 111369. https://doi.org/10.1016/j.biopha.2021.111369.
37. Silva DVT da, Baião D dos S, Ferreira VF, Paschoalin VMF. Betanin as a multipath oxidative stress and inflammation modulator: a beetroot pigment with protective effects on cardiovascular disease pathogenesis. *Crit Rev Food Sci Nutr*. 2020;0(0):1–16. https://doi.org/10.1080/10408398.2020.1822277.
38. Roopashree PG, Shetty SS, Suchetha Kumari N. Effect of medium chain fatty acid in human health and disease. *J Funct Foods*. 2021;87, 104724. https://doi.org/10.1016/j.jff.2021.104724.
39. Pinto A, Bonucci A, Maggi E, Corsi M, Businaro R. Antioxidant and anti-inflammatory activity of ketogenic diet: new perspectives for neuroprotection in alzheimer's disease. *Antioxidants*. 2018;7(5). https://doi.org/10.3390/antiox7050063.
40. Cenini G, Voos W. Mitochondria as potential targets in Alzheimer disease therapy: an update. *Front Pharmacol*. 2019;10(JULY):902. https://doi.org/10.3389/fphar.2019.00902.
41. Vandenberghe C, St-Pierre V, Pierotti T, Fortier M, Castellano CA, Cunnane SC. Tricaprylin alone increases plasma ketone response more than coconut oil or other medium-chain triglycerides: an acute crossover study in healthy adults. *Curr Dev Nutr*. 2017;1(4). https://doi.org/10.3945/cdn.116.000257.
42. de la Rubia Ortí JE, García-Pardo MP, Drehmer E, et al. Improvement of main cognitive functions in patients with alzheimer's disease after treatment with coconut oil enriched mediterranean diet: a pilot study. *J Alzheimers Dis*. 2018;65(2):577–587. https://doi.org/10.3233/JAD-180184.
43. Bolívar BE, Vogel TP, Bouchier-Hayes L. Inflammatory caspase regulation: maintaining balance between inflammation and cell death in health and disease. *FEBS J*. 2019;286(14):2628–2644. https://doi.org/10.1111/febs.14926.
44. Fenini G, Contassot E, French LE. Potential of IL-1, IL-18 and inflammasome inhibition for the treatment of inflammatory skin diseases. *Front Pharmacol*. 2017;8 (MAY):278. https://doi.org/10.3389/fphar.2017.00278.
45. Khan S, Ghouse HP. Role of NLRP3 inflammasome in alzheimer ' s disease. *Austin Publ*. 2015;2(3):1–6. https://austinpublishinggroup.com/clinical-neurology/fulltext/ajcn-v2-id1029.php. Accessed February 19, 2022.
46. Zhao Y, Dang M, Zhang W, et al. Neuroprotective effects of Syringic acid against aluminium chloride induced oxidative stress mediated neuroinflammation in rat model of Alzheimer's disease. *J Funct Foods*. 2020;71, 104009. https://doi.org/10.1016/j.jff.2020.104009.
47. Zhang H, Wang P, Yu H, et al. Aluminum trichloride-induced hippocampal inflammatory lesions are associated with IL-1B-activated IL-1 signaling pathway in developing rats. *Chemosphere*. 2018;203:170–178. https://doi.org/10.1016/j.chemosphere.2018.03.162.
48. Aboelwafa HR, El-Kott AF, Abd-Ella EM, Yousef HN. The possible neuroprotective effect of silymarin against aluminum chloride-prompted alzheimer's-like disease in rats. *Brain Sci*. 2020;10(9):1–21. https://doi.org/10.3390/brainsci10090628.
49. Cao Z, Wang P, Gao X, Shao B, Zhao S, Li Y. Lycopene attenuates aluminum-induced hippocampal lesions by inhibiting oxidative stress-mediated inflammation and apoptosis in the rat. *J Inorg Biochem*. 2019;193:143–151. https://doi.org/10.1016/j.jinorgbio.2019.01.017.
50. Jahn H. Memory loss in Alzheimer's disease. *Dialogues Clin Neurosci*. 2013;15(4):445–454. https://doi.org/10.4324/9780429314384-1.